IOSR Journal of Engineering (IOSRJEN) **www.iosrjen.org**
ISSN (e): 2250-3021, ISSN (p): 2278-8719
PP 49-55

Effect Of Ni^{2+} And Mg^{2+} Co-Doping On Structuraland Luminescent Properties Of Zns Nanoparticles

V. Venkatasubbian[a], R.Mohan[b*],C. Rakkappan[c] and N. Punitha[d] and K. Thamizharasan [e]

[a]*Department of Physics, S.B.K. College, Aruppukottai – 626101.*
[b*] *Department of Physics, School of Engineering and Technology, Surya Group of Institution Vikiravandi – 605 652*
[c] *Department of Physics, Annamalai University 608 002, Tamil Nadu, India.*
[d]*Department of Physics, St.Joseph's College of Engineering, Chennai – 600 119.*
[e] *Department of Physics, Sir Theagaraya College, Chennai – 600 021.*

Abstract: *ZnS nanoparticles codoped with Ni^{2+} and Mg^{2+} have been synthesized at room temperature through soft chemical route. The nanostructures of the prepared nanoparticles have been anlysised using X-ray diffraction (XRD), Scanning election microscope (SEM) with energy dispersive diffraction (EDX), UV-Vis spectrophotometer, PL spectrophotometer and Fourier transform infrared spectroscopy. The sizes of the as codoped nanoparticles are found to be 5.2 – 7.8 nm range. Room temperature photoluminescent spectrum exhibits multiple emission peaks under UV excitation. The Mg^{2+} doped ZnS:Ni^{2+} samples enhanced the visibile light emission at optimal concentration and there after concentration quenching effect was observed.*

Keywords: *Zinc sulfidecodoped with Ni^{2+} and Mg^{2+}; Nanoparticles; UV Visible - Photoluminescence; XRD; FESEM*

I. Introduction

Luminescence studies of nanomaterials showed that the physical properties of individual nanoparticles could be different from those of their bulk counterparts, originating from surface and quantum confinement effects [1]. Attention has been focused on luminescent compound semiconductor quantum dots of II–VI compounds because of the relative ease of synthesizing high quality materials using colloidal techniques [2–6]. Among the family of II–VI semiconductors, zinc sulfide (ZnS) is a technologically versatile and important semiconducting material for many photonic and optoelectronic applications, especially in nanocrystalline form [7].

Doping with optically active luminescent materials, the band-gap and the PL emissions in a wide range of wavelength in nanoparticles may be tailored by altering the impurity type, concentration and crystal dimensions. Semiconductor nanocrystals doped with different metal ions such as ZnS:Te, ZnS:Cu^{2+}, ZnS:Ni^{2+}, ZnS:Mn^{2+} show blue, green, orange, respectively [8–11]. These doped semiconducting nanocrystals can yield both high luminescence efficiencies and lifetime shortening from microseconds to nanoseconds at the same time. These spectacular results suggested that doped semiconductor nanocrystals form a new class of luminescent materials, with a wide range of applications in optoelectronic devices. Presence of two different kinds of ions simultaneously in a host material produces luminescence which is completely different from the emission due to single ion and this property is very beneficial for optoelectronic device applications. Recently, many researchers have tried to dope two different types of ions into the ZnSbased semiconductornanocrystals to tune their luminescent properties. However, there are very few reports on ZnS nanoparticles coactivated with Ni^{2+} and Mg^{2+} metallic ions.

Therefore, Ni^{2+} and Mg^{2+} co-dopants have been chosen as doping elements, unlike the previous studies, where the dopants are of different nature i.e., transition metal and rare earth metal respectively. It is very important to understand the nature of conduction and defect centers that these two different types of metallic elements create in the optical band gap [12–13]. In view of this, in the present study an attempt has been made to synthesize $Zn_{0.97-X}Ni_{0.03}Mg_XS$ nanoparticles with x = 0, 1, 2, 3, 4 and 5 % by the chemical route using PVP as surface capping ingredient. The roll of PVP is to passivate the surface atoms such that the energy levels inside the gap is eliminated so as to decrease the particle size.

II. Experimental Technique

A.R. grade with 99 % purity of Zinc acetate dihydrate [$Zn(CH_3COO)_2.2H_2O$], Nickel acetate dihydrate [$NiCH_3COO)_2.2H_2O$], Magnesium acetate dihydrate [$Mg(CH_3COO)_2.2H_2O$], sodium sulfide (Na_2S) and ethanol were used as reagents and Poly vinyl Pyrrolidone was used as capping agent. All chemicals are purchased from Merck India limited and used as received without further purification as they are analytical grade reagents. Ultrapure deionized water was used for aqueous solution preparation. The synthetic process of various polymers capped ZnS:Ni^{2+} nanoparticles flow chart is given in Fig. 2.1.

The X-ray diffraction (XRD) patterns were recorded to characterize the phase and structure of the Nps using X'PERT PRO diffractometer with Cu – Kα radiation (1.5406 Å) at 40 kv and 150 mA, 2θ range 20 - 80°. The particle size and structure were confirmed using a JEOL high resolution transmission electron microscope (HRTEM). The optical absorption spectra of all the samples in deionized water were analysised using SHIMADSU UV – Vis 117 double beam spectrophotometer.The photoluminescence measurements work was carried out on SHIMADZU RF 5301 PC spectroflurophotometer.

III. Structural Analysis

XRD patterns of the as synthesized $Zn_{0.97-x}Ni_{0.03}Mg_xS$ nanoparticles with different Mg concentrations (X = 0, 1, 3 and 5 %) are presented in Fig. 6.1. In all the samples, three dominant diffraction peaks positioned at 2θ = 28.98°, 49.06° and 57.02° could be indexed to the (111), (220), and (311) lattice planes of the cubic ZnS respectively, which match well with JCPDS card No. 05-0566. This shows that the cubic structure of the ZnS:Ni^{2+} samples is not affected by the Mg^{2+} substitution in the lattice and no secondary phases of metal clusters were observed in the XRD patterns. These results indicate that good crystalline and single phased $Zn_{0.97-x}Ni_{0.03}Mg_xS$ nanoparticles have been synthesized upto Mg concentration of 5 wt.%. The XRD spectra showed a shift of the diffraction peaks towards higher diffraction angle as the Mg co-doping concentration is increased. This shift evidenced the incorporation of Mg into the ZnS:Ni^{2+} lattice. The slight systematic shift may be due to the substitution of Zn^{2+} (ionic radius of 0.74 Å) by Mg^{2+} with a smaller ionic radius (0.72 Å). Furthermore, it is observed that the prominent peak intensity slightly decreased and the full width at half maximum (FWHM) slightly increased with increasing Mg co-doping concentration, which could be attributed to the lattice disorder created by the entry of Mg^{2+} atoms in the ZnS:Ni^{2+} lattice. The average nanocrystallite size (D) was calculated from the FWHM of the prominent (111) peak using Debye–Scherrer's formula,

$$D = \frac{0.9\lambda}{\beta Cos\theta} \quad (1)$$

where λ is wavelength of the Cu Kα irradiation, β is the FWHM of the diffraction peak and θ is diffraction angle for the (111) planes of cubic ZnS. The estimated crystallite sizes listed in Table 6.1, indicate a steady decrease of crystallite size with increasing Mg concentration. For ZnS, the grain growth is enhanced with higher density of Zn interstitials. In the present case of ZnS:Ni^{2+} nanoparticles, the Mg^{2+} co-doping reduces, the concentration of Zn in the lattice. As a result the density of Zn interstitial decreased, which reduced the diffusivity in ZnS:Ni^{2+} and the grain growth rate.

IV. Morphological Studies

The FESEM images (Fig. 6.2) clearly show that Mg^{2+} co-doped ZnS nanoparticles become more uniform than doped ones, and the sizes of the prepared ZnS samples have been significantly altered due to the incorporation of Mg^{2+} atoms. From the overall morphology of Mg^{2+} co-doped ZnS:Ni^{2+}, it can be noticed that the sample is composed of numerous nearly-monodispersed spherical structure with hollow nanospheres formed [16–19]. This indicates that the walls of the hollow nanospheres have a relatively high compactness and stability. The average particle size from the FESEM observation shows that the sphere consists of numerous tiny particles with the size of tens of nanometers within 200 to 300 nm.

The elemental analysis of ZnS:(Ni,Mg) nanoparticles was done by EDAX. Fig. 6.3 (a) and (b) show typical EDAX spectra of ZnS:Ni^{2+} and ZnS:Ni^{2+},Mg^{2+} nanoparticles, respectively. The spectra reveal that only the expected elements, Zn, S and Ni, are present in ZnS:Ni^{2+} and that in addition Mg^{2+} element exists in ZnS:Ni^{2+},Mg^{2+} samples. No traces of other elements were noticed in the spectra indicating the purity of the samples. The estimated Ni and Mg concentrations are near to stoichiometry indicating that most of the Ni and Mg ions exist in ZnS:Ni^{2+},Mg^{2+}nanocrystallites rather than in the form of hydroxides. However, the estimated dopant ion concentrations are slightly less than the nominal values indicating that some of the Ni and Mg ions still remained in the parent solution and had not been incorporated into the crystals. The relative error is less than ± 0.5%.

V. Optical Study

The absorption spectra of the samples are shown in Fig. 5. By introducing two metal ions into Zn Snanocrystallites, the band gap of the co-doped samples is different from that of doped sample. This is because of the difference between the localized energy level of excitation states of the composite center of Ni^{2+} and Mg^{2+} ions and that of the undoped sample. If the samples have a direct energy band gap, then their band gap can be approximated by the following formula [20–21]:

$$\alpha = \ln T \quad (2)$$

$$(\alpha h\nu)^2 = \left(h\nu - E_g\right) \quad (3)$$

where α is the absorption coefficient, T is the transmission coefficient, ν is the frequency of the transmission light, E_g is the band gap, and h is Planck's constant. This means that plots of $(\alpha\ h\nu)^2$ versus hν should be straight lines and the intercept on the hν axis give a value for the energy band gap Eg. Such plots are shown in Fig. 6.6. The straight lines imply that the $Zn_{1-x}Mg_xS$ samples have direct energy band gap and the band gap increased from 3.90 to 4.04 eV with the increase of Mg^{2+} concentration. This result is due to the larger band gap for MgS than ZnS. Also, in this work, the band gap of ZnS QDs (3.7 eV) was slightly larger than the reported ZnS bulk (3.66 eV), which is due to the quantum confinement effects as also suggested in Ref. [22]. \

VI. Spectral Analysis

To further ascertain, the surface properties of Ni doped ZnS and Mg co-doped ZnS:Ni^{2+} nanoparticles, the FTIR spectrum was recorded and shown in Fig. 6. Assignments of IR band frequencies of vibrational frequencies have been provided in Table 6.4. The obtained peak values are in good agreement with the reported values. It can be seen from Fig. 6 that there are clear variations in the positions and sizes of FTIR peaks representing Mg which might have been incorporated in ZnS:Ni^{2+} host [23–24]. A wide band in the region of 3447 cm^{-1} has been assigned to the stretching vibration mode of a hydroxyl group [25]. In the PVP capped Mg co-doped ZnS:Ni^{2+} nanoparticles, the absorption peaks at 2937 cm^{-1} correspond to C=O stretching. A broad absorption band at 1675 cm^{-1} due to coupled resonance, including a major contribution from C=O stretching along with some from C–N moiety (adjacent to carbonyl group). A sharp peak at a lower frequency, 1664 cm^{-1}, (Figure 6.8) which is due to interaction between the carbonyl group of pyrrolidone pendant of PVP and Zn^{2+}, results in lowering of C=O bond order. In plots for Mg co-doped ZnS:Ni^{2+}nanocrystallites, wide bands at 1343 cm^{-1} are attributed to the Mg-O stretching vibration while it is entirely absent in the undopedZnS sample. 1007 cm^{-1} is attributed to C=N stretching. The formation of co-ordinate bond between the nitrogen atom of the PVP and the Zn^{2+} ions is believed to be present.

VII. Conclusion

The co-dopants of different nature viz., rare earth and transition metal ions are incorporated in the ZnS system through colloidal chemical technique. The structural analysis of as synthesized samples revealed that the smaller ionic radius Mg^{2+} substitute the host lattice without disturbing the cubic structure of ZnS and further decrease the density of Zn interstitial, so that the grain growth is minimized. The morphological analysis through FESEM revealed that the co-doped samples are monodispersed in the form of hollow nanospheres. EDAX spectra confirms the presence of estimated Ni and Mg concentration in the ZnS lattice. The optical absorption studies revealed the increase in direct energy band gap due to quantum confinement effect.

Reference

[1] X. Zhang, H. Song, L. Yu, T. Wang, X. Ren, X. Kong, Y. Xie, X. Wang, J. Lumin. 118 (2006) 251.
[2] M. Wang, E.K. Na, J.S. Kim, E.J. Kima, S.H. Hahn, C. Park, K.-K. Koo, Mater. Lett.61 (2007) 4094.
[3] S.K. Mehta, S. Kumar, M. Gradzielski, J. Colloid Interface Sci. 360 (2011) 497.
[4] P. Reiss, New J. Chem. 31 (2007) 1843.
[5] V. Singh, P. Chauhan, J. Phys. Chem. Solids 70 (2009) 1074.
[6] M.S. Abd El-sadek, S. MoorthyBabu, Physica B 405 (2010) 3279–3283.
[7] R. Chen, D. Li, B. Liu, Z. Peng, G.G. Gurzadyan, Q. Xiong, H. Sun, Nano Lett. 10 (2010) 4956.
[8] S. Kim, T. Lim, M. Jung, K.-J. Kong, K.-S. An, S. Ju, J. Lumin. 130 (2010) 2153.
[9] W.Q. Peng, G.W. Cong, S.C. Qu, Z.G. Wang, Opt. Mater. 29 (2006) 313.
[10] P. Ya n g, M. Lu, D. Xu, D. Yuan, J. Chang, G. Zhou, M. Pan, Appl. Phys. A 74 (2002) 257.
[11] Q. Xiao, C. Xiao, Appl. Surf. Sci. 254 (2008) 6432.
[12] G. Goncalves, A. Pimentel, E. Fortunato, R. Martins, E.L. Queiroz, R.F. Bianchi, R.M. Faria, J. Non-Cryst.
[13] Solids 352 (2006) 1444.
[14] A.S. Fawzi, A.D. Sheikh, V.L. Mathe, J. Alloy. Compd. 502 (2010) 231.
[15] Kate Wright, Robert A. Jackson, J. Mater. Chem. 5 (1995) 2037.
[16] P. Bonasewicz, W. Hirschwald, G. Neumann, J. Electrochem. Soc. 133 (1986) 2270.
[17] J. Sun, G. Chen, Y. Feng and Y. Wang, RSC Advances, 4 (2014) 44466.
[18] Y. Liu, G. Xi, S. Chen, X. Zhang, Y. Zhu and Y. Qian, Nanotech. 18 (2007) 285605.
[19] X. Liu, X. Chen, X. Cui and R. Yu, Ceramics International, 40 (2014) 13847.

[20] M. Ashokkumar and S. Muthukumaran, Journal of Luminescence, 162 (2015) 97.
[21] Ogah E. Ogah, Guillaume Zoppi, Ian Forbes, R.W. Miles, Thin Solid Films 517 (2009) 2485.
[22] E.A. Dalchiele, P. Giorgi, R.E. Marotti, F. Martin, J.R.R. Barrado, R. Ayouci, D.Leinen, Solar Energy Mater.
[23] Solar Cells 70 (2001) 245.
[24] Y. Li, D. Yi, Y. Zhang, Y. Qian, J. Phys. Chem. Solids 60 (1999) 13.
[25] U. Senapati, D. Jha and D. Sarkar, Res. J. Physical Sci, 1 (2013) 1.
[26] P. Bandyopadhyay, A. Dey, R. Basu, S. Das and P. Nandy, Current Appli. Phys. 14 (2014) 1149.
[27] D. M. A. Raj, A. D. Raj, A. A. Irudayaraj, R. Josephine, M. S. Kumar and M. Thambidurai, J. Mater. Sci.:
[28] Mater.Electron. 26 (2015) 659.

Figure captions:

Fig. 1 XRD pattern of Ni^{2+} doped ZnS and Mg^{2+} co-doped ZnS:Ni^{2+} nanoparticles
Fig. 2: FESEM images of ZnS:Ni^{2+} and (b) Mg^{2+} co-doped ZnS:Ni^{2+} nanoparticles
Fig. 3: EDAX images of ZnS:Ni^{2+} and (b) Mg^{2+} co-doped ZnS:Ni^{2+} nanoparticles
Fig. 4: UV-Vis spectra of Ni^{2+} doped ZnS and Mg^{2+} co-doped ZnS:Ni^{2+} nanoparticles
Fig. 5:$(\alpha h\nu)^2$ vs. E_g for Ni^{2+} doped ZnS and Mg^{2+} co-doped ZnS:Ni^{2+} nanoparticles
Fig. 6. FTIR spectra of Ni^{2+} doped ZnS and Mg^{2+} co-doped ZnS:Ni^{2+} nanoparticles

Table captions:

Table 1 Structural parameters for Ni^{2+} doped ZnS and Mg^{2+} co-doped ZnS:Ni^{2+} nanoparticles

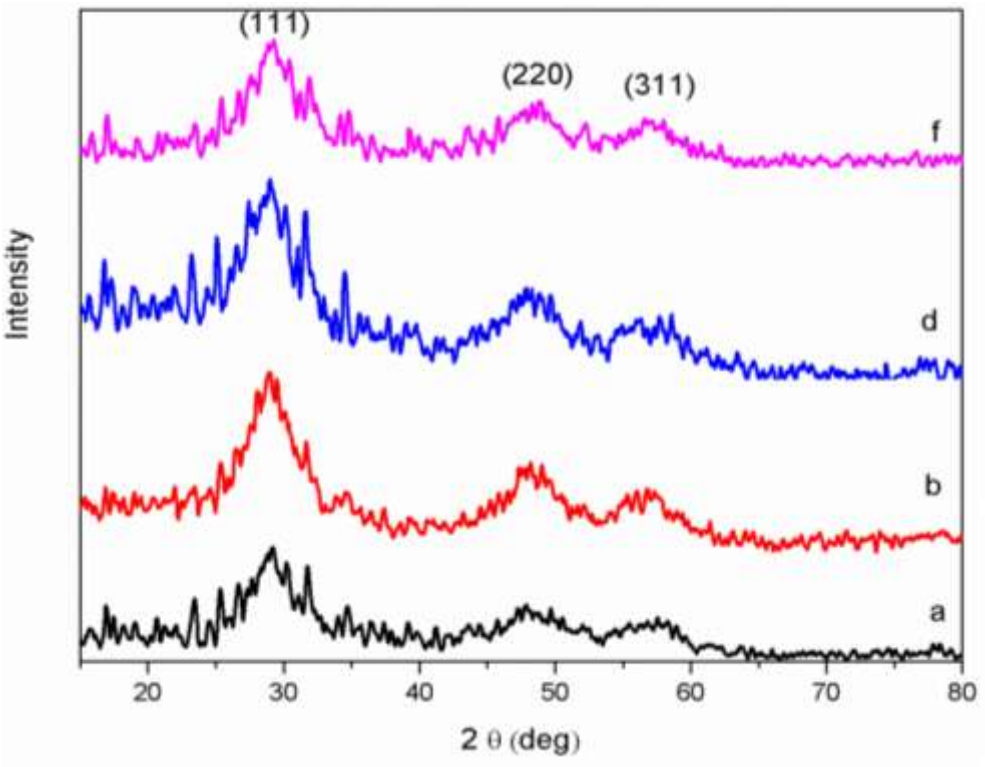

Fig. 1 XRD pattern of Ni^{2+} doped ZnS and Mg^{2+} co-doped ZnS:Ni^{2+} nanoparticles

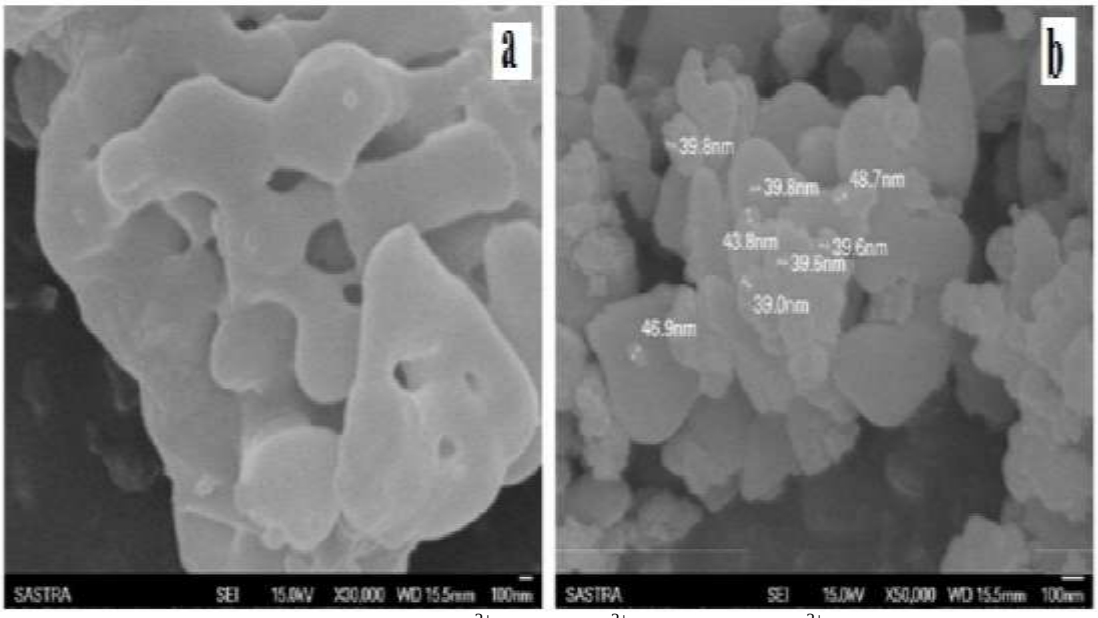

Fig. 2: FESEM images of ZnS:Ni^{2+} and (b) Mg^{2+} co-doped ZnS:Ni^{2+} nanoparticles

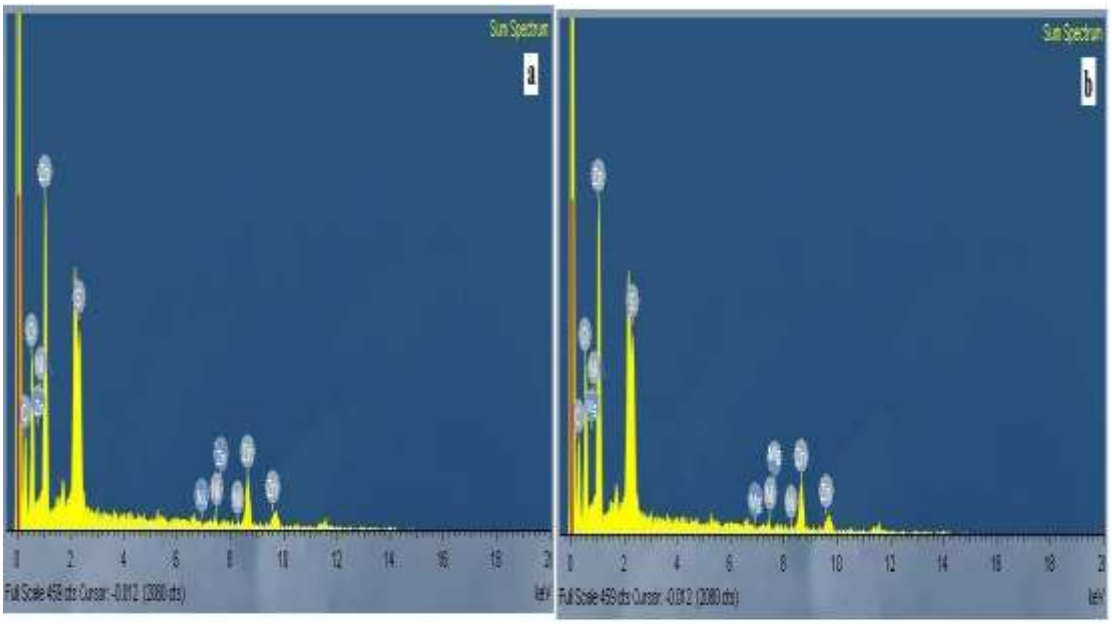

Fig. 3: EDAXimages of ZnS:Ni^{2+} and (b) Mg^{2+} co-doped ZnS:Ni^{2+} nanoparticles

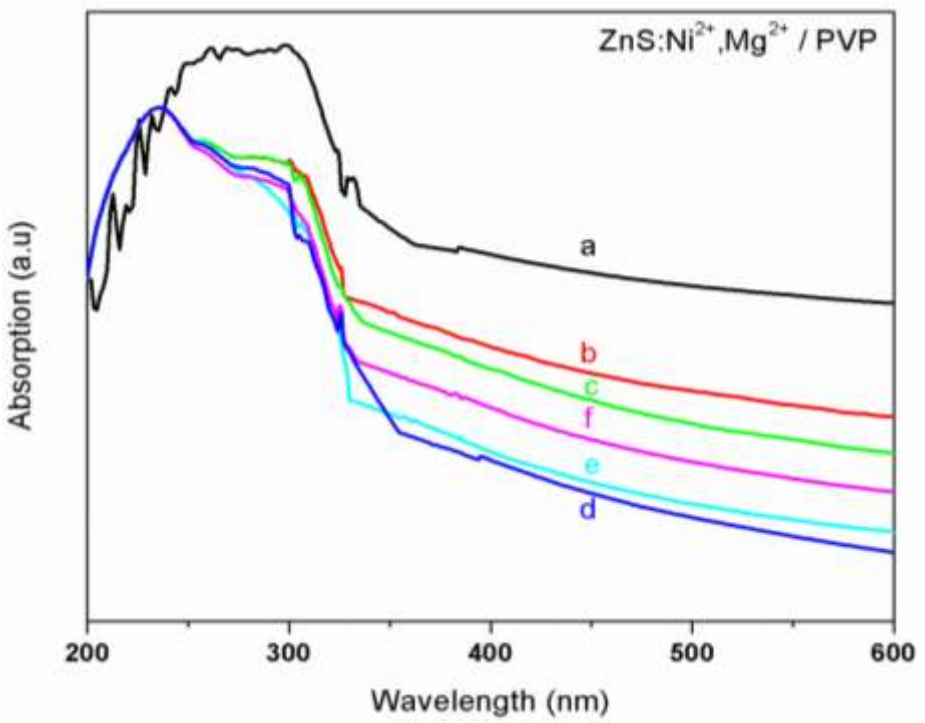

Fig. 4: UV-Vis spectra of Ni^{2+} doped ZnS and Mg^{2+} co-doped ZnS:Ni^{2+} nanoparticles

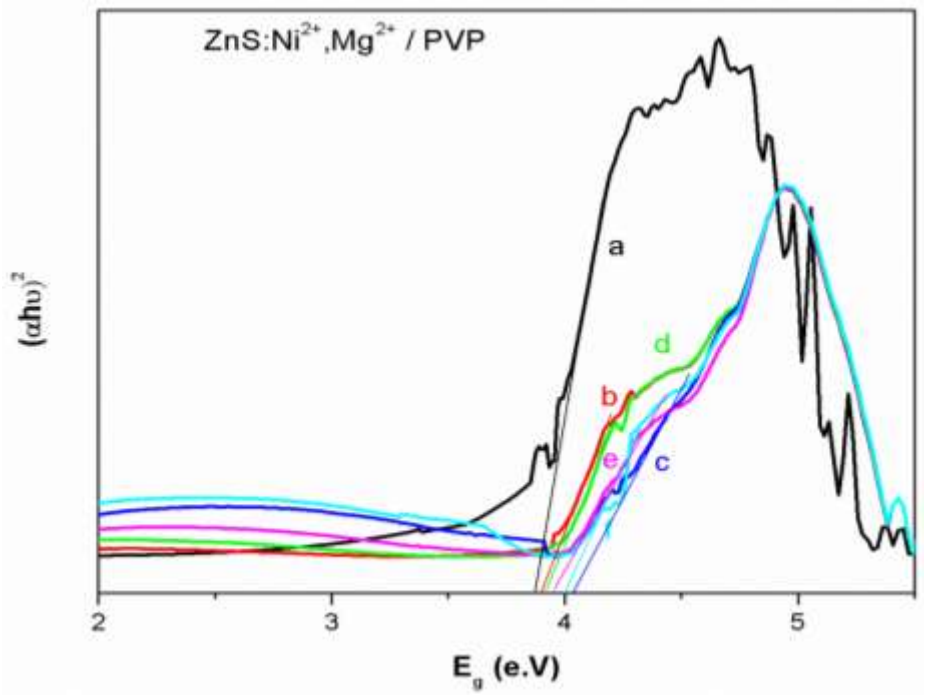

Fig. 5:$(\alpha h\nu)^2$ vs. E_g for Ni^{2+} doped ZnS and Mg^{2+} co-doped ZnS:Ni^{2+} nanoparticles

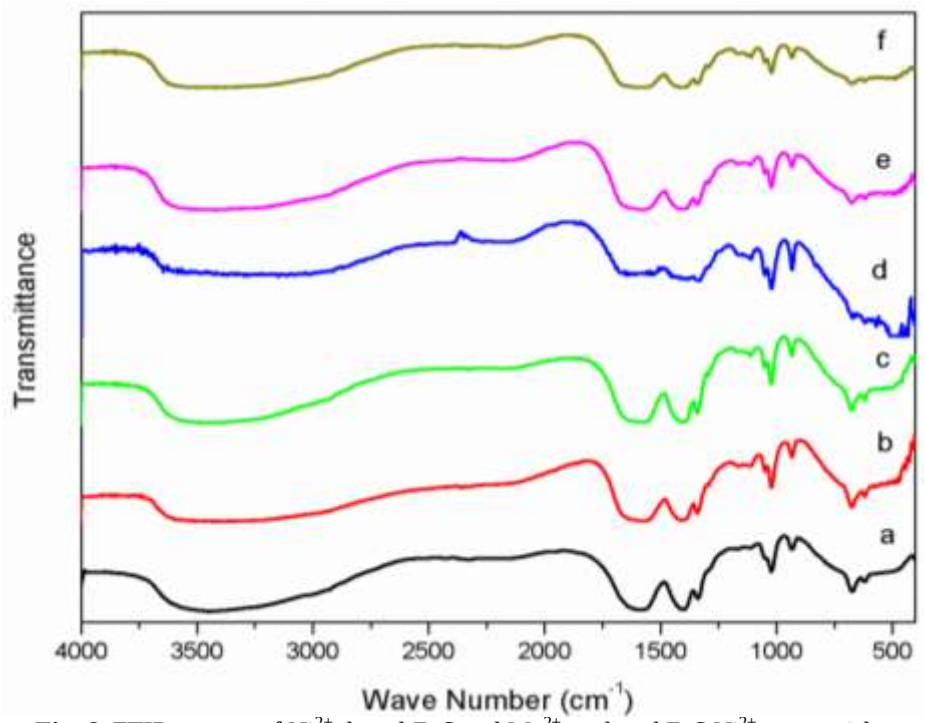

Fig. 6. FTIR spectra of Ni^{2+} doped ZnS and Mg^{2+} co-doped ZnS:Ni^{2+} nanoparticles

Sl.No	Name	d space	a Å	D Size	δ $10*10^{16}$lin/m^2	Sa $(nm)^2$	Vol $(nm)^3$	SA/Vol	SSA $10*10^6$ cm^2/g	ε
1	Pure ZnS	3.057	5.295	10.73	0.867	362.25	648.32	0.558	138.99	0.0134
2	ZnS:Ni^{2+}, Mg^{2+} 1%	3.17	5.491	7.895	1.604	195.76	257.56	0.757	188.9	0.0178
3	ZnS:Ni^{2+}, Mg^{2+} 3%	3.249	5.628	5.205	3.691	85.14	73.87	1.152	286.53	0.0277
4	ZnS:Ni^{2+}, Mg^{2+} 5%	3.226	5.588	5.562	3.232	97.18	90.09	1.078	268.14	0.0258